

NANO EXPRESS

Open Access



# Photovoltaic Characteristics of GaSe/MoSe<sub>2</sub> Heterojunction Devices

Ryousuke Ishikawa<sup>1\*</sup>, Pil Ju Ko<sup>2†</sup>, Ryoutaro Anzo<sup>3</sup>, Chang Lim Woo<sup>2</sup>, Gilgu Oh<sup>3</sup> and Nozomu Tsuboi<sup>3</sup>

## Abstract

The two-dimensional materials have the thickness of an atomic layer level and are expected as alternative materials for future electronics and optoelectronics due to their specific properties. Especially recently, transition metal mono-chalcogenides and dichalcogenides have attracted attention. Since these materials have a band gap unlike graphene and exhibit a semiconductor property even in a single layer, application to a new flexible optoelectronics is expected. In this study, the photovoltaic characteristics of a GaSe/MoSe<sub>2</sub> heterojunction device using two-dimensional semiconductors, p-type GaSe and n-type MoSe<sub>2</sub>, were investigated. The heterojunction device was prepared by transferring GaSe and MoSe<sub>2</sub> onto the substrate which the titanium electrodes were fabricated through a mechanical peeling method. The current–voltage characteristics of the GaSe/MoSe<sub>2</sub> heterojunction device were measured in a dark condition and under light irradiation using a solar simulator. The irradiation light intensity was changed from 0.5 to 1.5 sun. It was found that when the illuminance was increased in this illuminance range, both the short-circuit current and the open-circuit voltage increased. The open-circuit voltage and the energy conversion efficiency were 0.41 V and 0.46% under 1.5 sun condition, respectively.

**Keywords:** 2D materials, Heterojunction, Solar cell, GaSe, MoSe<sub>2</sub>

## Introduction

Two-dimensional (2D) materials have been found to have various unique characteristics that are not an extension of conventional materials science [1–5]. In particular, they are attracting attention as optoelectronic materials owing to the notable physical properties such as their strong optical absorption in the solar spectrum region [6], high internal radiative efficiencies [7], and tunable band gaps for both single- and multi-junction solar cells [8]. Some solar cells are made of 2D materials by forming in-plane and out-of-plane heterojunctions. The former is characterized in that a very clean heterojunction interface can be formed by continuously growing different types of 2D materials [9, 10]. On the other hand, in the latter case, since the heterojunction area can be increased, and tandem solar cells can be fabricated by

stacking several junctions, the solar cell characteristics of the GaSe/MoSe<sub>2</sub> vertical heterojunction device were evaluated in this study.

Gallium selenide has long been expected as an optical material for photodetectors and nonlinear optics, but its practical application has been promoted only in limited situations due to the difficulty of synthesizing single crystals [11–13]. However, due to recent advances in two-dimensional materials science, this layered optical material has been attracting attention again [14–21]. MoSe<sub>2</sub> is a typical transition metal dichalcogenide, the Mo ion in these compounds is surrounded by six Se<sup>2−</sup> ions. The coordination geometry of the Mo is found as octahedral and trigonal prismatic. Monolayer MoSe<sub>2</sub> exhibits semiconducting properties with a direct bandgap of about 1.6 eV and has relatively high carrier mobility on the order of hundreds [22]. Therefore, MoSe<sub>2</sub> is attracting attention not only as optoelectronics but also as an active region material for transistors [23, 24].

\*Correspondence: rishikaw@tcu.ac.jp

<sup>†</sup>Ryousuke Ishikawa and Pil Ju Ko have contributed equally to this work.

<sup>1</sup> Advanced Research Laboratories, Tokyo City University, Tokyo, Japan

Full list of author information is available at the end of the article

These 2D material heterojunctions have high potential as solar cell materials due to the properties already described that very high theoretical conversion efficiencies for single- and tandem-junctions have been demonstrated thanks to high external radiative efficiency [8], but conversion efficiencies reported so far due to inadequate material and interface quality and device design [25–27]. Furthermore, there are still many unclear points about the device physics in the out-of-plane heterostructure of 2D materials, especially the carrier separation process, which is important in solar cells.

In this paper, the current-voltage characteristics of the GaSe/MoSe<sub>2</sub> heterojunction device fabricated through a mechanical peeling method were measured in a dark condition and under light irradiation using a solar simulator. The irradiation light intensity was changed from 0.5 to 1.5 sun. It was found that when the illuminance was increased in this illuminance range, both the short-circuit current and the open-circuit voltage increased. The open-circuit voltage and the energy conversion efficiency were 0.41 V and 0.46% under 1.5 sun condition, respectively.

## Methods

We fabricated four-terminal devices using 50 nm of thickness titanium (Ti) electrodes deposited by electron-beam evaporation on p-type silicon substrates covered with 300 nm of thermally oxidized silicon dioxide (SiO<sub>2</sub>). We transferred flakes of natural GaSe and MoSe<sub>2</sub> (HQ graphene) onto the Ti electrodes sequentially using polydimethylsiloxane (PDMS, Dow Toray) by mechanical exfoliation as described in previous report [23]. Finally, the Ti/GaSe/MoSe<sub>2</sub> heterojunction device was annealed at 400 °C under nitrogen gas atmosphere for two hours. The transmittance and reflectance spectra in a few ten micro meters square

areas were obtained using transferred flakes onto glass substrates by a micro-UV–Vis spectrometer with a wide-band cassegrain objectives lens (JASCO MSV-5300). The thickness of each sample flakes was determined from line profile of atomic force microscopy (AFM) images (HITACHI Nano Navi Real). The micro-PL and Raman measurements were conducted with a continuous wave excitation laser emitting at 532 nm coupled to a 100× microscope objective at 25 °C. The excitation light intensities for Raman and PL measurements were 1.5 and 0.3 mW, respectively. The solar cell performance was measured at a sample temperature of 25 °C using a solar simulator with a variable intensity between 0.5 sun and 1.5 sun. The spectral response was evaluated by combining a monochromatic light source and a pico-ammeter. From the optical microscopic image, the heterojunction region was determined as the active area of solar cells.

## Results and Discussion

Figure 1a shows the transmittance (*T*) and reflectance (*R*) spectra of GaSe flake on glass substrates. The solid red and blue lines show the measured transmittance and reflectance spectra in the range of 200–1600 nm, respectively. The absorbance spectrum (*A*) represented by a solid black line was calculated by following relation;

$$A = 1 - T - R \quad (1)$$

The absorption coefficient was calculated by following equation as shown in Fig. 1b.

$$\alpha = \frac{\ln(1 - R) - \ln T}{d} \quad (2)$$

where *d* is thickness of sample, which was estimated to be  $638 \pm 29$  nm by AFM measurement. The absorption

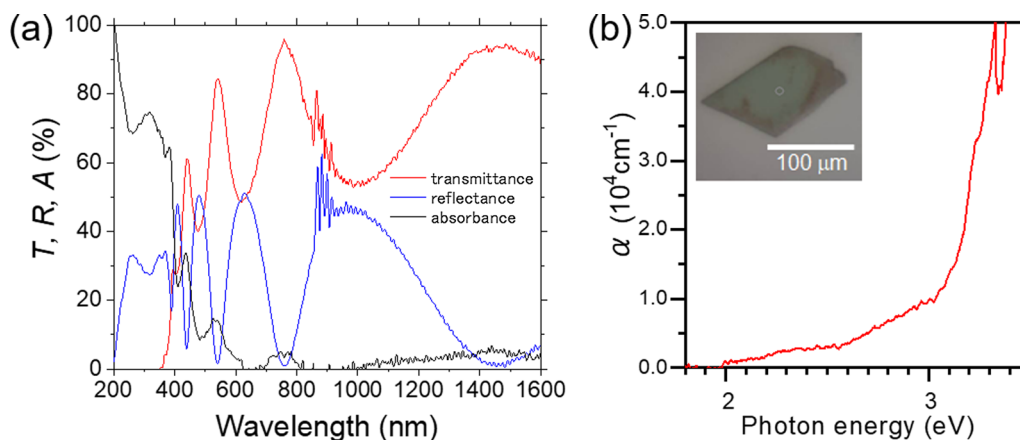


**Fig. 1** **a** Transmittance, reflectance, absorbance spectra and **b** absorption coefficient of GaSe flake. Inset: optical microscope image of GaSe flake

coefficient of GaSe gradually increased from around 2 eV corresponding to the bandgap. Since the valence band maximum exists at  $\Gamma$ -point, and the bottom of the conduction band at  $\Gamma$ -point is only a few tens meV above the conduction band minimum at M-point, GaSe is considered a quasi-direct bandgap [12]. Direct excitons are also known to be at the  $\Gamma$ -point of energy very close to the direct and indirect interband transitions [12, 19]. Inset of Fig. 1b shows the optical microscope (OM) image of GaSe flake for measurement. The centered circle in OM image indicates measuring area. On the other hand, Fig. 2 shows the optical properties of MoSe<sub>2</sub> flake with the thickness of  $99 \pm 3$  nm transferred on glass substrates. The absorption coefficient of MoSe<sub>2</sub> exhibited more than an order of magnitude higher than that of GaSe. The sharp increase from 1.5 eV and two exciton-oriented peaks were compatible to previous reports [28, 29].

Next, the crystallinity and further optical properties of these two-dimensional materials were investigated by Raman and PL. Raman and PL spectra were measured using fabricated GaSe/MoSe<sub>2</sub> heterojunction devices. The Raman peaks at 133, 214, and 309 cm<sup>-1</sup> were observed as shown in Fig. 3a. The Raman peaks at 133 and 309 cm<sup>-1</sup> indicate the planar vibrational modes of A<sup>1</sup><sub>1g</sub> (133 cm<sup>-1</sup>) and A<sup>2</sup><sub>1g</sub> (309 cm<sup>-1</sup>), respectively. The other peak at 214 cm<sup>-1</sup> comes from the vibration of selenides in the out-of-plane mode so called E<sup>1</sup><sub>2g</sub> [15, 17]. These clear crystalline vibrations indicate high crystallinity of transferred GaSe flakes. Figure 3b shows the PL spectrum obtained from GaSe flakes on Si substrate at 25 °C. The PL peaks around 626 and 655 nm corresponding to the direct and the indirect bandgaps, respectively. The indirect bandgap sets only 25 meV lower than the direct bandgap in GaSe [18, 19]. The Raman spectra of MoSe<sub>2</sub> transferred on Si substrates indicated two obvious peaks at around 236

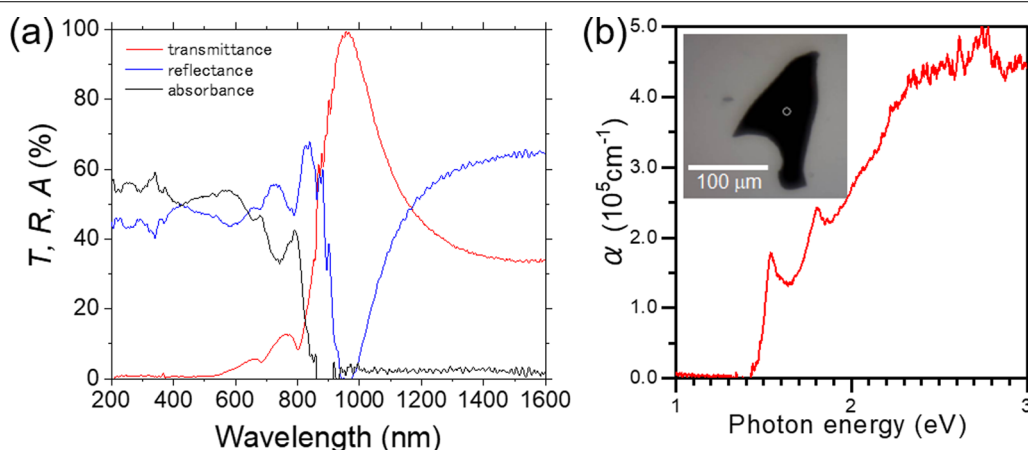


**Fig. 2** **a** Transmittance, reflectance, absorbance spectra and **b** absorption coefficient of MoSe<sub>2</sub> flake. Inset: optical microscope image of MoSe<sub>2</sub> flake

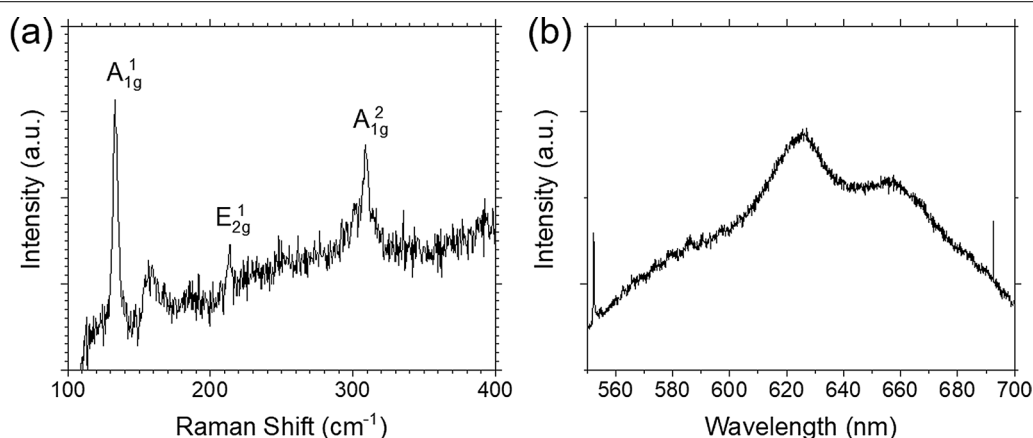


**Fig. 3** **a** Raman and **b** PL spectra of GaSe flake

and  $243\text{ cm}^{-1}$ , which are corresponding to  $A_{1g}$  mode as shown in Fig. 4a. The Raman and luminescence spectra (Fig. 4b) indicate high quality of transferred  $\text{MoSe}_2$  flakes on Si substrates.

Figure 5a shows the optical microscopic image of the fabricated  $\text{GaSe}/\text{MoSe}_2$  heterojunction device contacted with Ti electrodes. The  $\text{GaSe}$  flake is contacted with left and bottom electrodes, and the  $\text{MoSe}_2$  flake is contacted with right and top electrodes, respectively. The heterojunction region defined as the active area of solar cells was estimated to be  $490\text{ }\mu\text{m}^2$  from this image. The solar cell performance was measured using bottom and top electrodes under simulated sunlight. The thickness of these  $\text{GaSe}$  and  $\text{MoSe}_2$  flakes were estimated to be 118 and 79 nm by AFM measurement, respectively. Both of these film thicknesses correspond to 120–130 layers. Schematic image and band diagram of  $\text{GaSe}/\text{MoSe}_2$  heterojunction device were illustrated in Fig. 5b, c, respectively.

The current-voltage characteristics of the fabricated  $\text{GaSe}/\text{MoSe}_2$  heterojunction device under 0.5–1.5 sun light condition are shown in Fig. 6a. It is clear that this heterojunction device exhibits rectification and photovoltaic effect, and it can also be seen that the  $I$ – $V$  curve changes depending on the light irradiation intensity from Fig. 6a. Figure 6b shows a summary of the light irradiation intensity dependence of the short-circuit current ( $I_{sc}$ ) and the open-circuit voltage ( $V_{oc}$ ).  $I_{sc}$  increases linearly with light irradiation intensity in this range. On the other hand, it can be seen that  $V_{oc}$  increases logarithmically with respect to the light irradiation intensity. Since the following relational expression holds for an ideal diode, the ideal factor was estimated to be 1.11 by fitting.

$$V_{oc} = \frac{nk_B T}{q} \ln \left( \frac{I_L}{I_{dark}} + 1 \right) \quad (3)$$

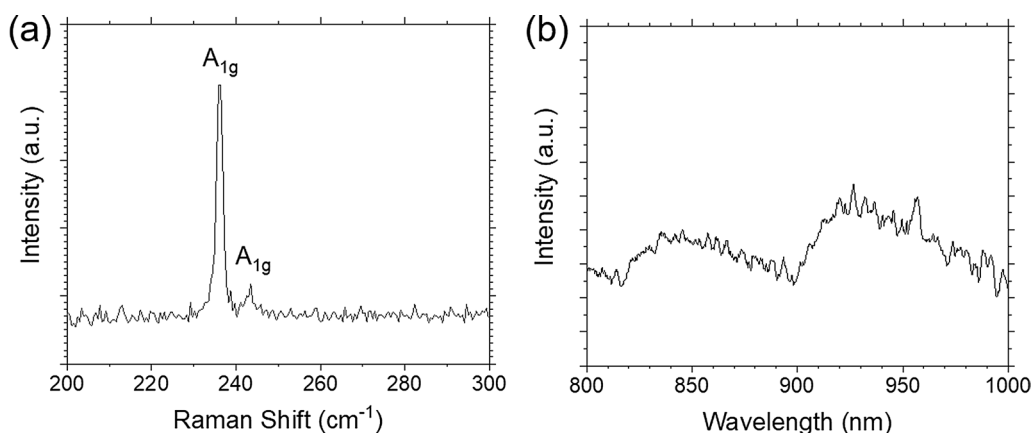


**Fig. 4** **a** Raman and **b** PL spectra of  $\text{MoSe}_2$  flake

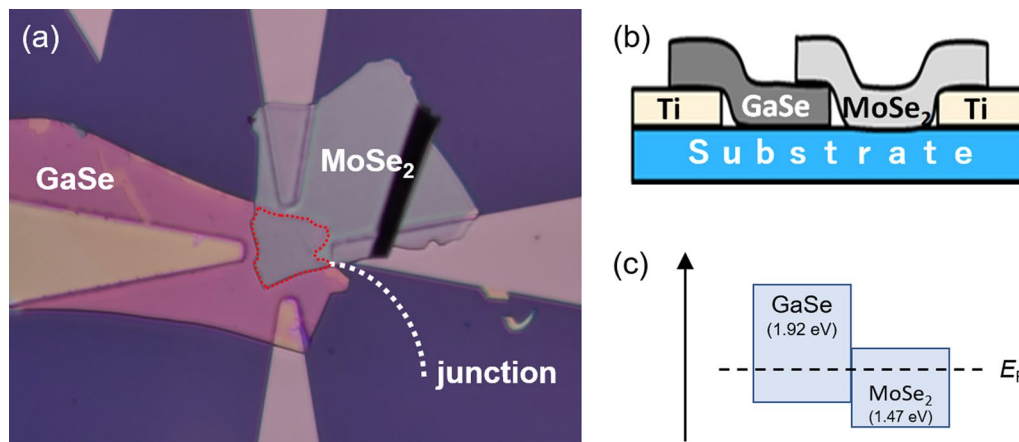
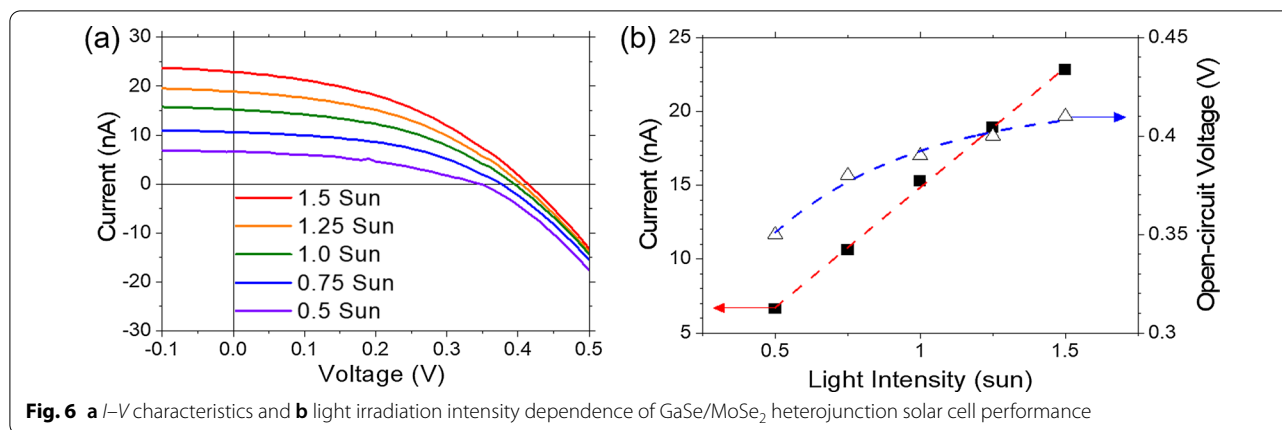
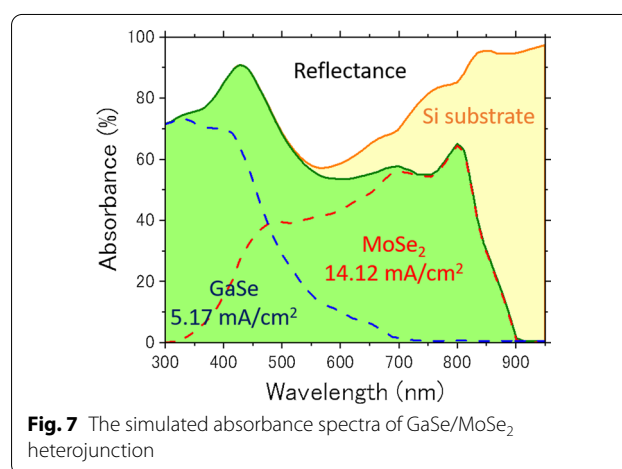


**Fig. 5** **a** Optical microscopic image, **b** schematic image, and **c** band diagram of the fabricated  $\text{GaSe}/\text{MoSe}_2$  heterojunction device



where  $n$  is the ideality factor,  $k_B$  is the Boltzmann constant,  $T$  is the temperature of the device,  $q$  is the fundamental unit of charge, so that  $\frac{k_B T}{q} \approx 0.0258$  V at room temperature. The  $I_L$  and  $I_{\text{dark}}$  are photo- and dark-current, respectively. An ideal factor closes to 1 indicates that this GaSe/MoSe<sub>2</sub> structure forms an ideal heterojunction in which an internal electric field sufficient to dissociate excitons is present. The short-circuit current density ( $J_{\text{sc}}$ ) was calculated to be 3.11 mA/cm<sup>2</sup> from active area defined by optical image. The fill factor ( $FF$ ) and conversion efficiency ( $\eta$ ) were estimated to be 0.44 and 0.54% under 1 sun condition, respectively. Since the  $FF$  decreased due to the influence of the series resistance when irradiating for 1 sun or more, the  $\eta$  was almost the same as when irradiating for 1 sun, although the  $J_{\text{sc}}$  and the  $V_{\text{oc}}$  increased. In order to improve  $FF$ , it is necessary to improve the device configuration such as shortening the distance to the electrode.

Next, we estimated the external quantum efficiency of the GaSe/MoSe<sub>2</sub> heterojunction by using an optical simulator (e-ARC) [29]. Calculations were made with a completely flat structure in which GaSe and MoSe<sub>2</sub> with the same film thickness as the fabricated device were laminated on a flat Si substrate. The optical constants of GaSe and MoSe<sub>2</sub> were referred to the reported values [30, 31]. The carrier loss induced by recombination at material interface and bulk regions are fully incorporated. The simulated absorbance spectra are shown in Fig. 7. The green-colored region shows the absorption region of the GaSe/MoSe<sub>2</sub> heterojunction, which is the sum of the absorption of GaSe indicated by the blue dashed line and the absorption of MoSe<sub>2</sub> indicated by the red dashed line. The yellow region is transmitted and absorbed by the Si substrate, and the other regions show reflection components. The maximum  $J_{\text{sc}}$  over the wavelength range of 300–950 nm was estimated to be 19.29 mA/cm<sup>2</sup> if the generated



photocarriers could be completely collected from fabricated device. Our simulation results predicted that the  $J_{\text{sc}}$  would increase, and 23 mA/cm<sup>2</sup> could be obtained when the GaSe film thickness was about 60 nm. The large dissociation between the calculated current value and the experimental value may be due to insufficient built-in potential in the fabricated device. If this hypothesis is correct, optimizing the film thickness of the absorbent layer and optimizing the work function of the contact material could significantly improve the  $J_{\text{sc}}$ . Furthermore, since this simulation result shows that the reflection component is also large, it can be said that the light confinement effect on the incident surface side and the back surface side of the GaSe/MoSe<sub>2</sub> heterojunction solar cell is also an important issue in the future. Surface plasmon technology is considered to be very effective for light confinement in two-dimensional material-based solar cells [32].

## Conclusions

In conclusion, we fabricated the GaSe/MoSe<sub>2</sub> heterojunction devices through a mechanical peeling method and analyzed the photovoltaic performance. The absorption coefficient obtained from transmittance and reflectance spectra of MoSe<sub>2</sub> exhibited more than an order of magnitude higher than that of GaSe. The Raman and luminescence spectra of GaSe and MoSe<sub>2</sub> indicated that high crystallinity maintained after device fabrication. Both the short-circuit current and the open-circuit voltage increased when the light intensity is increased from 0.5 to 1.5 sun. The open-circuit voltage and the energy conversion efficiency were 0.41 V and 0.46% under 1.5 sun condition, respectively. The maximum  $J_{sc}$  over the wavelength range of 300–950 nm was estimated to be 19.29 mA/cm<sup>2</sup> if the generated photocarriers could be completely collected from fabricated device from optical simulation study. The optimizing the film thickness of the absorbent layer and optimizing the work function of the contact material could significantly improve the  $J_{sc}$ . Furthermore, the light confinement effect on the incident surface side and the back surface side of the GaSe/MoSe<sub>2</sub> heterojunction solar cell is also an important issue in the future.

## Abbreviations

2D materials: Two-dimensional materials; AFM: Atomic force microscopy; OM: Optical microscope;  $I_{sc}$ : Short-circuit current;  $V_{oc}$ : Open-circuit voltage;  $J_{sc}$ : Short-circuit current density; FF: Fill factor.

## Acknowledgements

Not applicable.

## Authors' contributions

CLW and PJK fabricated the devices. RA and GO characterized the devices. RI, NT, and PJK gave the idea and the experimental guidance for the whole processes and drafting the manuscript. All authors read and approved the final manuscript.

## Funding

This study was supported by the Japan Society for the Promotion of Science KAKENHI (Grant No. JP20H02851).

## Availability of Data and Materials

The datasets supporting the conclusions of this article are included within the article.

## Declarations

## Competing interests

The authors declare that they have no competing interests.

## Author details

<sup>1</sup>Advanced Research Laboratories, Tokyo City University, Tokyo, Japan. <sup>2</sup>Department of Electrical Engineering, Chosun University, Gwangju, Republic of Korea. <sup>3</sup>Department of Materials Science and Technology, University of Niigata, Niigata, Japan.

Received: 13 August 2021 Accepted: 20 November 2021

Published online: 29 November 2021

## References

- Geim AK, Grigorieva IV (2013) Van der Waals heterostructures. *Nature* 499:419–425
- Zeng H, Dai J, Yao W et al (2012) Valley polarization in MoS<sub>2</sub> monolayers by optical pumping. *Nat Nanotechnol* 7:490–493
- Cao T, Feng J, Shi J et al (2011) Valley-selective circular dichroism of monolayer molybdenum disulphide. *Nat Commun* 3:1–5
- Cao Y, Fatemi V, Fang S et al (2018) Unconventional superconductivity in magic-angle graphene superlattices. *Nature* 556:43–50
- Tran K, Moody G, Wu F et al (2019) Evidence for moiré excitons in van der Waals heterostructures. *Nature* 567:71–75
- Mak KF, Lee C, Hone J et al (2010) Atomically thin MoS<sub>2</sub>: a new direct-gap semiconductor. *Phys Rev Lett* 105:136805
- Amani M, Lien DH, Kiriya D et al (2015) Near-unity photoluminescence quantum yield in MoS<sub>2</sub>. *Science* 350:1065–1068
- Jariwala D, Davoyan AR, Wong J, Atwater HA (2017) Van der Waals materials for atomically-thin photovoltaics: promise and outlook. *ACS Photonics* 4:2962–2970
- Gong Y, Lin J, Wang X et al (2014) Vertical and in-plane heterostructures from WS<sub>2</sub>/MoS<sub>2</sub> monolayers. *Nat Mater* 13:1135–1142
- Kobayashi Y, Yoshida S, Maruyama M et al (2019) Continuous heteroepitaxy of two-dimensional heterostructures based on layered chalcogenides. *ACS Nano* 13:7527–7535
- Bube RH, Lind EL (1959) Photoconductivity of gallium selenide crystals. *Phys Rev* 115:1159–1164
- Mooser E, Schlüter M (1973) The band-gap excitons in gallium selenide. *Il Nuovo Cimento* 18:164–208
- Singh NB, Suhre DR, Balakrishna V et al (1998) Far-infrared conversion materials: gallium selenide for far-infrared conversion applications. *Prog Cryst Growth Charact Mater* 37:47–102
- Jappor HR, Habeeb MA (2018) Optical properties of two-dimensional GaS and GaSe monolayers. *Physica E* 101:251–255
- Hu P, Wen Z, Wang L et al (2012) Synthesis of few-layer GaSe nanosheets for high performance photodetectors. *ACS Nano* 6:5988–5994
- Ko PJ, Abderrahmane A, Takamura T et al (2016) Thickness dependence on the optoelectronic properties of multilayered GaSe based photodetector. *Nanotechnology* 27:325202
- Li X, Lin MW, Lin J et al (2016) Two-dimensional GaSe/MoSe<sub>2</sub> misfit bilayer heterojunctions by van der Waals epitaxy. *Sci Adv* 2:e1501882
- Pham KD, Phuc HV, Hieu NN et al (2018) Electronic properties of GaSe/MoSe<sub>2</sub> and GaS/MoSe<sub>2</sub> heterojunctions from first principles calculations. *AIP Adv* 8:075207
- Budweg A, Yadav D, Grupp A et al (2019) Control of excitonic absorption by thickness variation in few-layer GaSe. *Phys Rev B* 100:045404
- Pham KD, Nguyen CV, Phung HTT et al (2019) Strain and electric field tunable electronic properties of type-II band alignment in van der Waals GaSe/MoSe<sub>2</sub> heterostructure. *Chem Phys* 521:92–99
- Ning J, Zhou Y, Zhang J et al (2020) Self-driven photodetector based on a GaSe/MoSe<sub>2</sub> selenide van der Waals heterojunction with the hybrid contact. *Appl Phys Lett* 117:163104
- Tongay S, Zhou J, Ataca C et al (2012) Thermally driven crossover from indirect toward direct bandgap in 2D Semiconductors: MoSe<sub>2</sub> versus MoS<sub>2</sub>. *Nano Lett* 12:5576–5580
- Abderrahmane A, Ko PJ, Thu TV et al (2014) High photosensitivity few-layered MoSe<sub>2</sub> back-gated field-effect phototransistors. *Nanotechnology* 25:365202
- Larentis S, Fallahazad B, Tutuc E (2012) Field-effect transistors and intrinsic mobility in ultra-thin MoSe<sub>2</sub> layers. *Appl Phys Lett* 101:1–4
- Jariwala D, Sangwan VK, Lauhon LJ et al (2014) Emerging device applications for semiconducting two-dimensional transition metal dichalcogenides. *ACS Nano* 8:1102–1120
- Jariwala D, Davoyan AR, Tagliabue G et al (2016) Near-unity absorption in van der Waals semiconductors for ultrathin optoelectronics. *Nano Lett* 16:5482–5487



27. Wong J, Jariwala D, Tagliabue G et al (2017) High photovoltaic quantum efficiency in ultrathin van der Waals heterostructures. *ACS Nano* 11:7230–7240
28. Beal AR, Knights JC, Liang WY (1972) Transmission spectra of some transition metal dichalcogenides. II. Group VIA: trigonal prismatic coordination. *J Phys C Solid State Phys* 5:3540–3551
29. Arora A, Nogajewski K, Molas M et al (2015) Exciton band structure in layered  $\text{MoSe}_2$ : from a monolayer to the bulk limit. *Nanoscale* 7:20769–20775
30. Nakane A, Tampo H, Tamakoshi M et al (2016) Quantitative determination of optical and recombination losses in thin-film photovoltaic devices based on external quantum efficiency analysis. *J Appl Phys* 120:064505
31. Hsu C, Frisenda R, Schmidt R et al (2019) Thickness-dependent refractive index of 1L, 2L, and 3L  $\text{MoS}_2$ ,  $\text{MoSe}_2$ ,  $\text{WS}_2$ , and  $\text{WSe}_2$ . *Adv Opt Mater* 7:1900239
32. Nootchanat S, Pangdam A, Ishikawa R et al (2017) Grating-coupled surface plasmon resonance enhanced organic photovoltaic devices induced by Blu-ray disc recordable and Blu-ray disc grating structures. *Nanoscale* 9:4963–4971

### Publisher's Note

Springer Nature remains neutral with regard to jurisdictional claims in published maps and institutional affiliations.

**Submit your manuscript to a SpringerOpen<sup>®</sup> journal and benefit from:**

- Convenient online submission
- Rigorous peer review
- Open access: articles freely available online
- High visibility within the field
- Retaining the copyright to your article

---

Submit your next manuscript at ► [springeropen.com](https://www.springeropen.com)

---